Calibration of long-term geostationary infrared observations using HIRS

Kenneth R. Knapp
NOAA/National Climatic Data Center, Asheville, NC, 28801

Date of Submission:

_____

Submitted to:
Journal of Atmospheric and Oceanic Technology

_____

Kenneth R. Knapp
National Climatic Data Center
151 Patton Ave
Asheville, NC 28801-5001
828-271-4339 (voice)
828-271-4328 (fax)
Ken.Knapp@noaa.gov

Abstract

Infrared window (~11μm) brightness temperatures from global geostationary meteorological instruments were calibrated using the High-resolution Infrared Radiation Sounder (HIRS) instrument. The calibration was performed as an independent analysis of the satellite inter-calibration performed by the International Satellite Cloud Climatology Project (ISCCP) to ensure temporal and inter-satellite stability. However, criteria for matching geostationary observations with HIRS from previous literature were found to be inadequate due to the limited range of temperatures which passed the criteria. The result was an inability to determine the impact of a calibration error on observations of high clouds. To better understand the calibration error, a new set of matchup criteria which collected targets at all temperatures proportionately showed a significant shift in the ISCCP calibration. Using the new criteria, it became apparent that observations of cold temperatures were biased low. A correction based on these results removed the bias between the geostationary and HIRS observations. The calibration shift was attributed to a change in the Advanced Very High Resolution Radiometer (AVHRR) Level 1B Global Area Coverage (GAC) data format that inadvertently truncated calibration coefficients. Future calibrations of operational products should make use of multiple reference sensors to avoid potential calibration shifts and data providers should thoroughly document the impacts of changes in data formats for better data stewardship.

1. The need for satellite inter-calibration

Infrared observations from operational geostationary satellites have been made since the 1970s and allowed the generation of numerous operational weather products. These observations are also important for understanding climate, given their temporal and spatial coverage. For instance, the International Satellite Cloud Climatology Project (ISCCP) has shown that the international geostationary constellation can be used to monitor the distribution of clouds (Rossow and Schiffer, 1999). More recently, geostationary infrared observations have been used to reassess historical global tropical cyclone trends (Kossin *et al.*, 2006).

For climatic purposes, however, understanding the accuracy and precision of these measurements is equally important as the measurements themselves. All instruments in the ISCCP have on-board calibration sources for the infrared sensors. Yet, without inter-satellite calibration, boundaries appear at image seams and spurious trends appear in temporal and spatial series. Hence, the ISCCP project has endeavored to understand the calibration by inter-calibrating between geostationary satellites and polar-orbiting instruments. On a monthly basis, ISCCP normalizes the geostationary observations with each other to remove inter-satellite biases. ISCCP then performs an absolute calibration that ties the calibration for a particular month to a reference polar-orbiting satellite, currently the National Ocean and Atmospheric Administration (NOAA)-9 Advanced Very High Resolution Radiometer (AVHRR). More information on the ISCCP calibration is provided by Desormeaux et al. (1993) and Brest et al. (1997). The ISCCP calibration ensures temporal stability of the absolute calibration which is vital to climate applications. Herein, we performed an independent analysis of the ISCCP calibration using a new ISCCP data set and different reference instrument.

2. Scope of analysis

Studies exist which inter-compare observations from geostationary (GEO) imagers and polar orbiting instruments. However, this study differs three ways: the calibration reference source, the data set being calibrated, and the calibration targets.

First, the High-resolution Infrared Radiation Sounder (HIRS) was the reference calibration source instead of the AVHRR. While the comparison between brightness temperatures from GEO instruments and HIRS are not new (e.g., Gunshor *et al.*, 2004: Tian *et al.*, 2004), ISCCP has traditionally calibrated using AVHRR. Herein, HIRS was selected since co-locations will allow future calibration of the infrared water vapor channels in addition to the infrared window. Also, the HIRS spatial footprint of ~20 km allows averaging some pixels to overcome the low dynamic resolution (8-bit) GEO data (see below). The calibration correction derived here is directly applicable to the ISCCP coefficients but the method and corrections could be applied to the original satellite calibration or other radiometer matchups as well.

Second, this independent ISCCP calibration analysis used a global geostationary data set: ISCCP B1 data. The B1 data result from an initial spatial and temporal sub-sampling performed by the ISCCP data providers. These data have been archived since 1983 but have had little use until recent efforts at the National Climatic Data Center (NCDC) rediscovered the data format and navigation (Knapp, 2006). The data derive from nineteen GEO imagers flown worldwide from 1983 to 2005 from three satellite series: the Geostationary Operational Environmental Satellite (GOES), Geostationary Meteorological Satellite (GMS) and the European Meteorological Satellite's Meteosat. This work is an effort to make them temporally homogeneous and minimize inter-series differences.

Third, this effort is different in its calibration target: both cold and warm emitting surfaces. Previous studies emphasized clear-sky (i.e., warm) targets which, given the view zenith angle limitations, restricted most targets to warm Equatorial land and ocean. That, however, represented a small range of temperatures, especially when extrapolating to colder targets such as the cumulonimbus cloud tops of thunderstorms and hurricanes. As shown here, deriving calibration from a wider range of temperatures provided more stability at colder temperatures.

3. ISCCP B1 data

In spite of the number of satellites in the ISCCP B1 data, the observations are quite similar. In addition to GOES, GMS, and Meteosat, ISCCP B1 data can and will include other satellite series as they become available (e.g., the Chinese Fengyun-2C satellite). B1 data have been subsampled in time and space to 3-hour and 10-km and have 8-bit dynamic resolution. The coverage of the Earth (Figure 1) is nearly global (except for the Poles) which was accomplished by moving satellites to cover failures (e.g., GOES-6, 7, 9 and Meteosat-3) and previously unavailable regions (i.e., Meteosat-5 to 63° East longitude).

While observations from other channels are available in the B1 record, infrared window (IRWIN) observations are available from all satellites in the B1 data set. The IRWIN brightness temperature observations are vital in cloud cover, tropical cyclones and other climate variables. The IRWIN channel is generally centered near 11 μm which is a region of the atmospheric spectrum with little molecular absorption. In general there are two types of spectral response functions (SRF) for IRWIN channels (Figure 2): a broad (i.e., ~2 μm width) and narrow channel (~1 μm width). The broader channels (e.g., GMS-3, GOES-5 and the Meteosat series) are characteristic of the older instruments, when sensor noise was decreased by receiving more radiation. But this broader band has more atmospheric contamination due to water vapor

absorption. In contrast, newer instruments incorporated sensors with less noise allowing for a narrower IRWIN and another channel near 12μm: the split-window channel (e.g., GOES-8 through 11). The impact of the spectral differences between the IRWIN channels is important when comparing to a reference instrument with its own spectral response.

4. HIRS observations: A stable reference

The HIRS instrument is an atmospheric sounder which has been flown on the NOAA-series of satellites since 1978. For this study, we compared the brightness temperature observations by HIRS channel 8 (T_{HIRS}) from the HIRS all-sky Pathfinder data (Jackson *et al.*, 2003) with those from the ISCCP B1 IRWIN channels (T_{GEO}). The HIRS channel 8 SRF varied little during the satellite series (Figure 2): the central wavelength of channel 8 ranges from 11.11 to 11.15μm. Hence, the HIRS observations from satellite-to-satellite should be stable. The stability is demonstrated by the time series of the daily-average T_{HIRS} shown in Figure 3. Some inter-satellite variation might be expected due to orbital drift, but there is little difference between the series. Furthermore, Cao et al. (2005) studied the inter-satellite bias through simultaneous nadir observations near the poles for NOAA 15,16 and 17. For channel 8, the intersatellite difference was approximately 0.25K. Clearly, the HIRS channel 8 is a stable reference channel which is appropriate for use in calibrating T_{GEO} observations. However, how should one expect T_{HIRS} to differ from T_{GEO}?

5. How HIRS and GEO observations should vary

Given the differences in the spectral responses of the HIRS and the various GEO instruments their observations do vary from each other. These differences are primarily due to absorption and re-emission of water vapor above the emitting surface. Gunshor (2004) calculated

clear-sky brightness temperature differences between NOAA-14/HIRS and various GEO observations using a standard tropical atmosphere; differences ranged from -1.0 to +0.3K. Since we were interested in colder temperatures, we performed a similar analysis but included the potential for clouds.

The Santa Barbara Discrete Ordinate Radiative Transfer (DISORT) Atmospheric Radiative Transfer (SBDART) model (Ricchiazzi *et al.*, 1998) was used to calculate the brightness temperature differences between all the available GEO instruments and an average HIRS channel 8 SRF (the variations in temperature due to the HIRS SRF variations were small). Two emitting surfaces were simulated: the ground and a thick cloud at altitudes ranges from 1 to 13 km (thus, simulating 14 separate emitting altitudes). To simulate the varying amounts of water vapor in the atmosphere, the ground and cloud-top emissions were transmitted through three SBDART standard atmospheres: tropical and mid-latitude summer and winter. Brightness temperatures were calculated by integrating the modeled top-of-the-atmosphere radiation by the instrument SRF. Calculations were performed for nadir and 60° view zenith angles, which represent air masses of 1 and 2, respectively. Results are shown in Figure 4.

The differences between T_{GEO} and T_{HIRS} among the three series show similar tendencies. Overall, the differences vary from zero to 1.3K and generally increase with increasing temperature, suggesting that clear skies should have the largest differences. Also, while there is some increase in the differences by view zenith, the changes are small, primarily because both GEO and HIRS had a similar but not identical dependence on view zenith angle. And while there is some variation by satellite series, the tendency (of differences to asymptotically decrease with decreasing temperature) is apparent and consistent across most satellites. The GMS-series shows the largest intra-series variation but is not too different from the other series for temperatures

below 260K. In short, T_{GEO} should be no more than 1.3 K colder than T_{HIRS} with differences asymptotically decreasing with temperature. Also, differences between HIRS and GEO are similar in magnitude to the inter-satellite HIRS differences of 0.25K. Therefore, the HIRS channel 8 is an excellent reference for the ISCCP B1 calibration because it varies little between series, has small expected differences from T_{GEO} and is available for the entire ISCCP B1 record.

6. Determining sensor matchups

The HIRS and GEO brightness temperature observations are made from separate platforms in distinct orbits with different spatial resolutions. Thus, careful calculations are needed to ensure both systems are observing the same target. Tian et al. (2004) simply expanded the GEO data field of view to 5 × 5 pixels (approximately 55×55km) to approximate the HIRS footprints. Gunshor et al. (2004) smoothed both data sets to roughly 100-km resolution in search of large, uniform clear sky areas. Our approach was a bit more technical. In short, the Earth locations (i.e., latitudes and longitudes) of the ISCCP B1 pixels were calculated. View vectors from the location of the HIRS sensor in space to the Earth locations were then calculated. The angle between these B1 view vectors and a given a HIRS view vector define whether the B1 pixel falls within that HIRS footprint. Those B1 pixels within or near the HIRS field-of-view limit of 1.25° (Kidder and Vonder Haar, 1995) and occurring within 30 minutes of each other were averaged and stored in matchup files. In this way, the average values from the GEO observations were spatially equivalent to the HIRS footprint.

a. Where earlier filters fail

However, other matchup criteria were required to compare observations between a GEO and HIRS. Initially, the limits described by Tian at al (2004) were used (Table 1) where the

emphasis was to ensure that both systems observed the same target from the same geometry. The spatial distribution of the matchups using this initial filter is shown in Figure 5. For the 23 years of ISCCP B1 data, there are more than 6 million matchups (fewer matchups are available for the Indian Ocean because of the lack of a geostationary satellite for most of the period of record, cf. Figure 1). The spatial distribution is limited by the restrictions on the view zenith angle and azimuth angle differences which limits most of the calibration targets to tropical areas.

The monthly bias differences between T_{GEO} and T_{HIRS} are provided in Figure 6. In general, there is a positive bias for all GEO satellites primarily ranging from 0 to 2K. Also, there is evidence of a calibration shift in 2001 across all satellite series with another shift possible in 2005. This calibration shift was investigated and is described later. It is also interesting to note that the bias differences show less temporal variation from 1995 through 2001, with more variation in the earlier period (particularly the GMS series).

To determine the effect of the bias variations on colder targets (i.e., cloud top temperatures), linear regression was used to analyze the calibration variation. The T_{HIRS} values were linearly regressed against T_{GEO} on a monthly basis using the initial filter. The deviation of the linear regression from one-to-one is plotted versus T_{GEO} in Figure 7a. The values represented by the lines correspond to the difference of T_{GEO} from T_{HIRS} and act as an estimate of a calibration correction. The correction shows more variation at colder temperatures (e.g., T_{GEO}<220K) than at warmer ones. In fact, the corrections are clearly different for T_{GEO} ~300K during two time periods (i.e., before and after October 2001). Because of the variation at the colder temperatures, the effect of the 2K shift in 2001 on cold targets was not clear. Therefore, another matchup filter was needed to better estimate the effect of the calibration shift.

b. A proportionate filter for matchups

The convergence of the calibration correction lines in Figure 7a at warmer temperatures suggests that the bulk of the calibration points are at warmer temperatures. A two-dimensional histogram (Figure 8a) for a month of matchups confirms this. Figure 8 shows that the bulk of the matchups occur at warmer targets having lower spatial standard deviations of T_{GEO} within the HIRS footprint (σ_T). The 1K cutoff for noise from the initial filter (Tian *et al.*, 2004) removed disproportionately too many cold targets. This was partly due to the dynamic resolution of the ISCCP B1 data. ISCCP observations were sampled to 8 bits so a one-count difference corresponded to ~½K at 300K but ~1K change at 200K. That is, for the same radiance noise, T_{GEO} noise appeared greater for colder targets than warmer targets. This is further shown by comparing histograms (Figure 8b) of the matchups with different filters. While the matchups are distributed from 200 to 300K, the initial filter removed most targets with temperatures colder than 280 K.

A proportionate filter which kept more matchups at colder temperatures was proposed to increase the certainty of the calibration shift on cold targets. The hypothesis was that the matchups with the smoothest spatial distributions are better calibration targets and that fixed thresholds remove disproportionately too many cold observations. Instead of using fixed thresholds from the initial filter, the matchups were sorted by T_{GEO} into 10K bins. Matchups in the lowest 10^{th} percentile of spatial noise from each bin were kept as the best calibration targets. An example of the proportionate filter for August 1998 between NOAA-12 and GOES-8 is represented by the stepped line in Figure 8a. For warmer temperatures, the proportionate filter is stricter than the simple 1K threshold of the initial filter and is more relaxed for colder temperatures. The corresponding distribution of matchup temperatures (10K stepped line in

223 Figure 8b) is more representative of the entire range of brightness temperatures from the
224 matchups.

225 The initial filter was further modified by objectively redefining the limits on the matchup
226 parameters. In short, a large set of matchups were collected, linear regression was calculated, and
227 then variations from the linear regression were grouped by various matchup parameters. An
228 example of this analysis is shown in Figure 9 for August 1998 matchups between NOAA-
229 12/HIRS and GOES-8. First, the large set of matchups were used to compute linear regression
230 statistics (Figure 9a); in this case there were more than one million points, a correlation
231 coefficient (r) of 0.96, bias of 2.3K and a stand error of estimate (ε) of 4.2K. At this point, the
232 only filter is the 30-minute limit on the difference in observations times. The differences from
233 the linear regression were then grouped by various parameters (Figure 9b-e) to objectively
234 determine appropriate filter limits. For instance, there was little trend in the bias or RMS
235 difference versus time so the temporal limit was extended from the initial limit of ±15 min to
236 ±30 minutes between the HIRS and GEO observations. Conversely, there was a significant trend
237 in the bias for differences in the instrument view zenith angles (θ) so the initial filter on air mass
238 ($1/\cos\theta < 0.05$) was retained. The dependence of the error on azimuth angle differences,
239 however, was weak. While there is a peak at 90°, it is a residual of the locations of these
240 matchups and they are few in number. Since there was little azimuthal dependence and IR
241 radiation is generally azimuthally independent, the azimuth limit of the initial filter was
242 removed. Finally, the RMS difference increases with increasing spatial inhomogeneity (Figure
243 9e) but, more importantly, the bias has little to no trend. Since the proportionate filter limits
244 noise by using the smoothest (i.e., spatial standard deviation) 10% of matchups in each 10K
245 grouping of target temperatures, it will not likely incorporate bias by doing so. The resulting

246 proportionate filter limits are summarized in Table 1. The matchups passing the proportionate
247 filter are shown in Figure 8f where: r=0.997, bias=0.75K and ε=1.25K for 18,561 points. The
248 spatial distribution of these points is shown in Figure 10. In general, the matchups fall in limited
249 locations due to the sun-synchronous orbit combined with limitations on viewing and temporal
250 differences. However, for all satellites and months (Figure 11), the distribution of calibration
251 targets is more globally-distributed than the initial filter and the number of matchup points has
252 increased six-fold. Now the matchups are grouped near homogenous targets such as the
253 persistent stratus clouds east of North and South America.

254 The calibration matchups using the proportionate filter showed greater stability at colder
255 temperatures. For example, applying the proportionate filter to all GOES-10 matchups (Figure
256 7b) clearly distinguishes the three time periods identified from the bias difference time series
257 (Figure 6). The effect of the calibration shift is clear from the greater stability at colder
258 temperatures. For all time periods, the negative bias (i.e., T_{GEO}-T_{HIRS}) increases with decreasing
259 T_{GEO}, which is contrary to theory (cf. Figure 4). It became clear that the change in 2001 caused
260 the slope of the lines to be even steeper during the Oct. 2001-Dec.2004 time period. The result
261 implies that cold clouds were ~4K too cold and warm surfaces were ~2K too warm. It is also
262 interesting to note that the bias differences for 2005 (Figure 6) return to near zero, suggesting an
263 error was corrected. However, only through analyzing Figure 7b does it become clear that while
264 the bias at warm temperatures (T_{GEO}~300K) decreased, the differences at colder temperatures
265 were of the same magnitude as before: ~4K too cold. That is, while warmer temperatures are
266 closer, the slopes of the lines were similar to the previous period (Oct-2001 through Dec-2004).

267 After the calibration shift in the ISCCP data was discovered, its source was identified.
268 The step in calibration in 2001 resulted from a change in the NOAA Level 1B format for

AVHRR data. ISCCP switched the morning satellite (the satellite to which the absolute calibration is "tied") from NOAA-14/AVHRR to NOAA-16/AVHRR between September and October 2001. What was uncovered here is an artifact of that switch. Beginning with NOAA-15, the NOAA Level 1B GAC format began including the 2nd order non-linear correction in the calibration header. This allowed users to derive a more complete correction directly from the calibration header. However, the 2nd order coefficient was incorrectly truncated in the Global Area Coverage (GAC) header data. When ISCCP switched from NOAA-14 to NOAA-16, it unknowingly began using a truncated calibration coefficient. On 28 April 2005 the GAC data format was updated to the version 3 format which now contains accurate coefficients. Hence, the error stemmed from the nonlinear correction, which had a greater effect at the colder temperatures. Nonetheless, it is still unclear why the slopes in 2005 (green lines in Figure 7b) did not return to their pre-2001 values. This suggests that other issues in the ISCCP calibration may also need to be investigated. Nonetheless, since the calibration shift results in differences larger than that suggested by theory (<1K), a calibration correction was applied.

7. Correcting calibration differences

Calibration correction to the ISCCP absolute calibration was applied based on the analysis of the proportionate filter results. T_{GEO} was corrected using the slope and offset from the monthly comparisons with T_{HIRS}. The linear regression correlation, slope and offset for GOES-10 of the combined matchups are the squares in Figure 12. First, monthly correlations were used to determine months which might have matchup errors. The errors generally result from mis-navigated imagery or bad data and cause incorrect slope and offsets. Therefore, months with correlations less than 0.99 or less than two standard deviations from the mean monthly correlation were not used. This may have possibly removed "good" points, but the subsequent

temporal averaging minimized the effect. Removing a good point had less effect than keeping a bad point. Second, assuming that inter-monthly variations should be small and smooth, temporal averaging was applied to monthly slope and offset values. A fifth-order binomial average was applied to the slope and offset and is depicted by the thick gray line in Figure 12. However, the temporal average was not applied at the abrupt change in calibration occurring between September and October 2001. Lastly, T_{GEO} was corrected using the smoothed monthly slope and offset values.

The result of this correction is consistently small differences between T_{HIRS} and T_{GEO}. Using the corrected calibration, the variations of the monthly GOES-10 calibrations from one-to-one are nearly completely removed (Figure 13) from the previous comparisons (cf. Figure 7). Also, the bias differences (Figure 14) for all satellites are much smaller and more consistently near zero than with the initial filter (Figure 6) or the proportionate filter (not shown).

8. Discussion

The corrected calibration shows little bias when compared to HIRS and has allowed the data to be used to investigate trends in tropical storm intensity (Kossin *et al.*, 2006). While the effort here was to ensure that a temporally continuous record was available for climate analysis, certainly more could be done to investigate the differences. Nonetheless, the implications of this work are broad.

Calibration between satellites should attempt to obtain the bias difference at multiple target temperatures, instead of a small range (e.g., clear sky). The impact of not doing so, as shown here, is a poor understanding of the impact of a calibration shift on the entire range of target temperatures. Only after stabilizing the calibration using the proportionate filter did it become clear that a shift occured in 2001 and 2005. Also, limits on calibration matchups should

be performed objectively (as shown here) by examining the impact of the parameters on the resulting comparison. Arbitrarily choosing strict values unnecessarily limits the number of the matchups, which could weaken the significance of the comparisons with the reference instrument. Also, operational calibration should include intercomparisons among many reference satellites instead of just one. In doing so, a change in a reference satellite system can be caught sooner.

Finally, broader implications of this work apply to stewardship of the data. The simple application of these suggestions applies directly to deriving climate data records. However, the impact of a simple data format change was shown to impact ISCCP observations that are a vital component of global cloud observations. This emphasizes the importance of data stewardship not only in processing the data, but in simply recording and archiving data and the processes used to make the observations. Our understanding of climate will hinge on the quality of, not only the data itself, but also the data describing how the data are observed, recorded, modified and archived.

9. Conclusions

A satellite inter-calibration between geostationary imagers and the HIRS instrument was conducted and these are the key findings:

- HIRS provides stable observations with small expected differences from GEO observations
- These differences vary between GEO satellite series and decrease with temperature.
- Simple threshold filters used to matchup GEO observations with HIRS can be inadequate to analyze calibration across the range of observed temperatures.

- Shifts in the ISCCP calibration were found to cause cold targets to appear too cold (by ~4K) and warm targets to appear too warm (by ~2K).
- The ISSCP calibration error was attributed to a data format change in the raw AVHRR data.

Acknowledgements

The author acknowledges discussions with Bill Rossow, Darren Jackson, Lei Shi and John Bates.

References

Brest, C. L., W. B. Rossow, and M. D. Roiter, 1997: Update of Radiance Calibrations for ISCCP. *Journal of Atmospheric and Oceanic Technology*, **14,** 1091-1109.

Cao, C., H. Xu, J. Sullivan, L. McMillin, P. Ciren, and Y.-T. Hou, 2005: Intersatellite Radiance Biases for the High-Resolution Infrared Radiation Sounders (HIRS) on board NOAA-15, -16, and -17 from Simultaneous Nadir Observations. *Journal of Atmospheric and Oceanic Technology*, **22,** 381-395.

Desormeaux, Y., W. B. Rossow, C. L. Brest, and G. G. Campbell, 1993: Normalization and Calibration of Geostationary Satellite Radiances for the international Satellite Cloud Climatology Project. *Journal of Atmospheric and Oceanic Technology*, **10,** 304-325.

Gunshor, M. M., T. J. Schmit, and W. P. Menzel, 2004: Intercalibration of the Infrared Window and Water Vapor Channels on Operational Geostationary Environmental Satellites Using a Single Polar-Orbiting Satellite. *Journal of Atmospheric and Oceanic Technology*, **21,** 61-68.

Jackson, D. L., D. P. Wylie, and J. J. Bates, 2003: The HIRS Pathfinder Radiance data set (1979-2001). *AMS Conference on Satellite Meteorology and Oceanography*.

Kidder, S. Q. and T. H. Vonder Haar, 1995: *Satellite Meteorology: An Introduction*. Academic Press, Inc, 466 pp.

Knapp, K. R., 2006: Scientific Data Stewardship: Lessons learned from a satellite data rescue effort. *Bulletin of the American Meteorological Society*, **Submitted**.

362 Kossin, J. P., K. R. Knapp, D. J. Vimont, and R. J. Murnane, 2006: A Reanalysis of Global
363 Hurricane Trends. *Science*, **Submitted**.

364 Ricchiazzi, P., S. Yang, C. Gautier, and D. Sowle, 1998: SBDART: A Research and Teaching
365 Software Tool for Plane-Parallel Radiative Transfer in the Earth's Atmosphere. *Bulletin of the*
366 *American Meteorological Society*, **79,** 2101-2114.

367 Rossow, W. B. and R. A. Schiffer, 1999: Advances in Understanding Clouds from ISCCP.
368 *Bulletin of the American Meteorological Society*, **80,** 2261-2287.

369 Tian, B. J., B. J. Soden, and X. Q. Wu, 2004: Diurnal cycle of convection, clouds, and water
370 vapor in the tropical upper troposphere: Satellites versus a general circulation model. *Journal of*
371 *Geophysical Research-Atmospheres*, **109**.
372
373

Figure captions

Figure 1 - Temporal and spatial Equatorial coverage from the geostationary satellites which make up ISCCP B1 data (shading is limited to a view zenith angle less than 60°).

Figure 2 – Normalized IR window channel spectral response functions for the instruments in the ISCCP B1 data set and channel eight of the 10 HIRS instruments used (far right).

Figure 3 - Time series of daily-averaged HIRS channel 8 brightness temperatures from NOAA satellites 6 (N06) through 17 (N17).

Figure 4 - Theoretical differences in temperature between HIRS and GEO observations as a function of geostationary temperature for view zenith angles (θ) of 0° and 60° (top and bottom row, respectively).

Figure 5 – Geographical distribution of all matchup locations (from 1983 through 2005) using the initial filter (Table 1).

Figure 6 - Bias difference between T_{GEO} and T_{HIRS} for each satellite-month grouped by satelite series using the initial matchup filter.

Figure 7 – Difference from the one-to-one line for monthly linear regressions of T_{GEO} from GOES-10 with T_{HIRS} for a) initial matchup filtering, b) matchup using proportionate filter and c) corrected ISCCP calibration derived using the proportionate filter. In all plots, blue lines are for months prior to October 2001, red lines are from Oct. 2001 through December 2004 and green lines are months during 2005.

Figure 8 - a) Two-dimensional probability distribution function of August 1998 matchups between NOAA-12/HIRS and GOES-8 by geostationary noise (σ_T) and T_{GEO}. Solid line at 1K represents the initial filter limit and the stepped line represents the new proportionate filter limit.

b) Normalized distribution of temperature for all matchups (solid line, 1K bins), initial filter (dashed line) and the proportionate filter (solid line 10K bins).

Figure 9 – a) T_{GEO} versus T_{HIRS} for all matchup points between NOAA-12/HIRS and GOES-8 for August 1998. b-e) Distribution of RMS (thick line) and bias (thin) differences for all points (black line) and the proportionate filter (gray line) for difference in b) time, c) view zenith angle (θ), d) relative azimuth angle () and e) spatial noise of the HIRS observations (σ_T). f) T_{GEO} versus T_{HIRS} from the proportionate filter.

Figure 10 – Spatial distribution of matchup locations for points in Figure 9f using the proportionate filter.

Figure 11 - Scatter plot between T_{GEO}-T_{HIRS} and T_{GEO} for points in Figure 10, linear regression is dashed.

Figure 12 - Same as Figure 5 for proportionate filter (Table 1).

Figure 13 - Time series of linear regression correlation, slope and offset for proportionate-filtered monthly matchups between HIRS and GOES-10 infrared window channel. Months with a correlation above 0.99 were used (solid circles in slope and offset) in the temporal smoothing (gray line) to produce the final calibration correction for the slope and offset values.

Figure 14 – Same as Figure 7 except now using the corrected calibration (blue lines for months before October 2001 are plotted below red and green lines).

Figure 15 - Bias for all geostationary satellites and all months available after calibration correction based on the proportionate filter (cf. Figure 6).

Tables

Table 1 - Limits on the matchup criteria for the initial and proportionate filters.

Criteria	Initial Filter	Proportionate filter
Time	$\Delta t < 15$ min	$\Delta t < 30$ min
Noise	$\sigma(T_{GEO}) < 1$ K	$10\%^{ile}$ per 10K bin of T_{GEO}
View zenith	$\Delta[(\cos\theta)^{-1}] < 0.05$	$\Delta[(\cos\theta)^{-1}] < 0.05$
View azimuth	$\Delta\phi < 30°$ when $\theta > 5°$	None

Figures

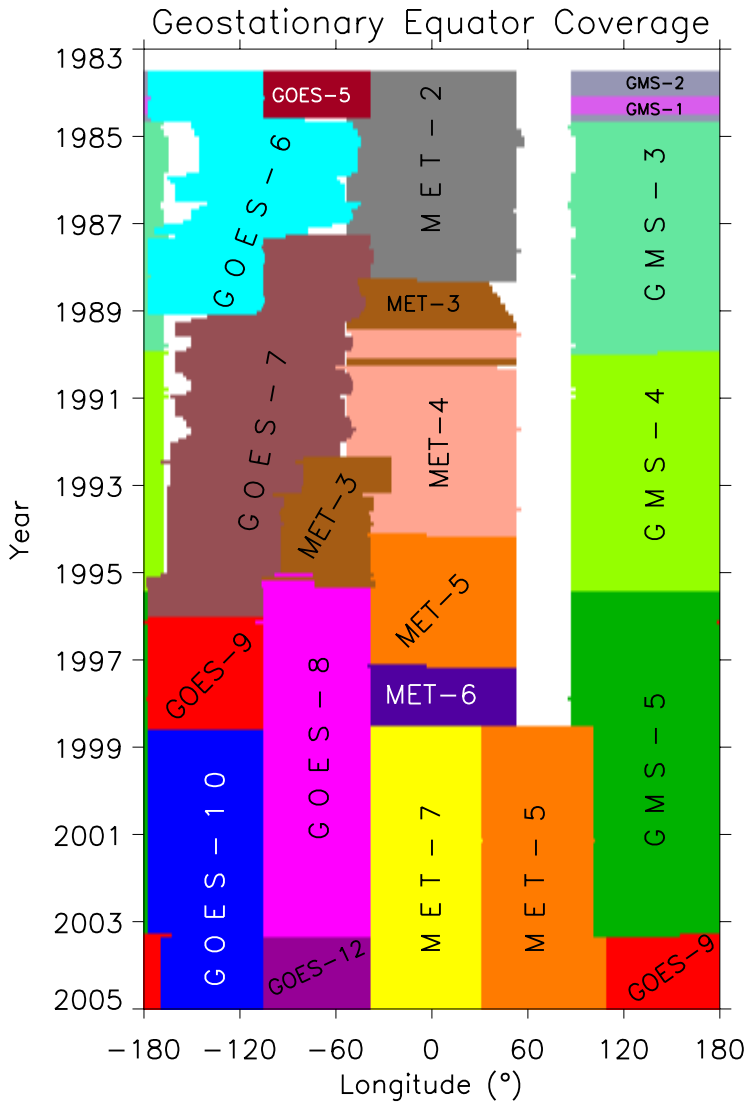

Figure 1 - Temporal and spatial Equatorial coverage from the geostationary satellites which make up ISCCP B1 data (shading is limited to a view zenith angle less than 60° for illustrative purposes).

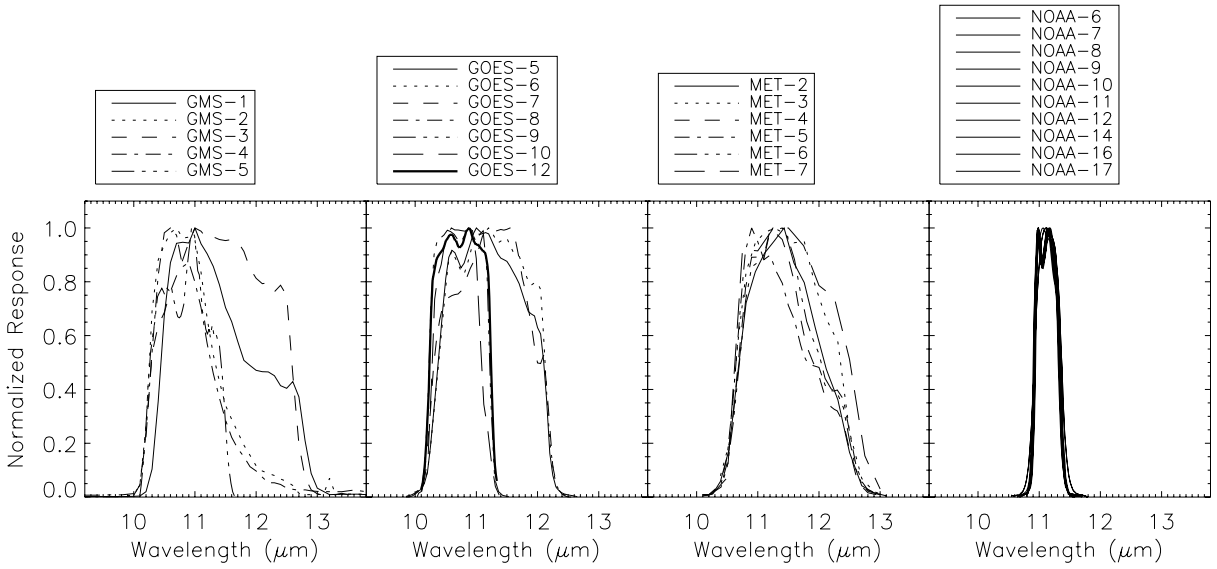

Figure 2 – Normalized IR window channel spectral response functions for the instruments in the ISCCP B1 data set and channel eight of the 10 HIRS instruments used (far right).

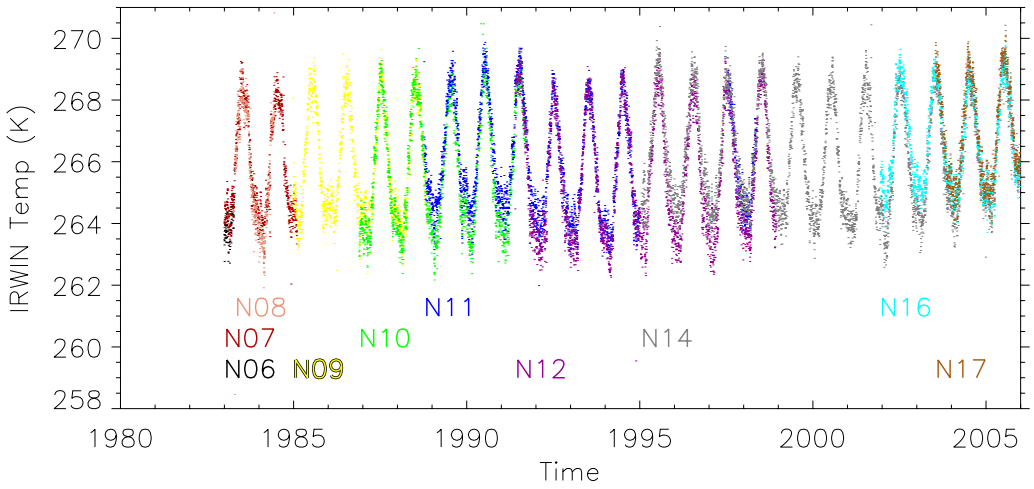

Figure 3 - Time series of daily-averaged HIRS channel 8 brightness temperatures from NOAA satellites 6 (N06) through 17 (N17).

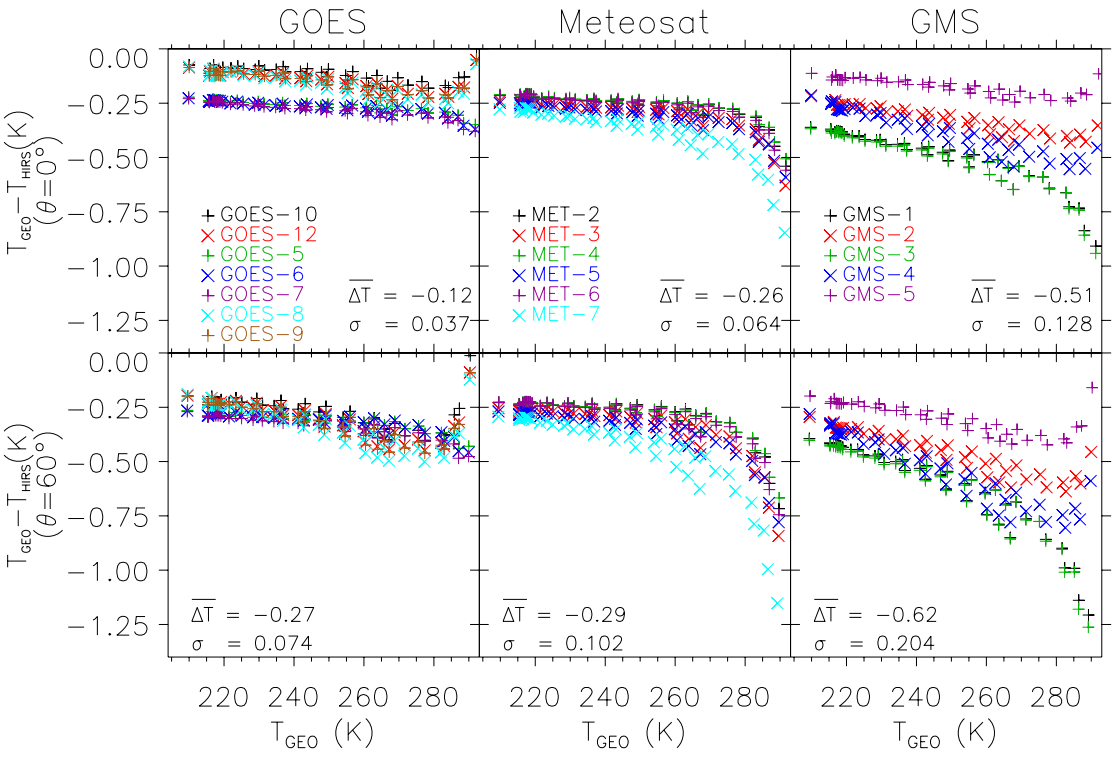

435

436 **Figure 4 - Theoretical differences in temperature between HIRS and GEO observations as**

437 **a function of geostationary temperature for view zenith angles (θ) of 0° and 60° (top and**

438 **bottom row, respectively). Series average (ΔT) and standard deviation (σ) are also**

439 **provided.**

440

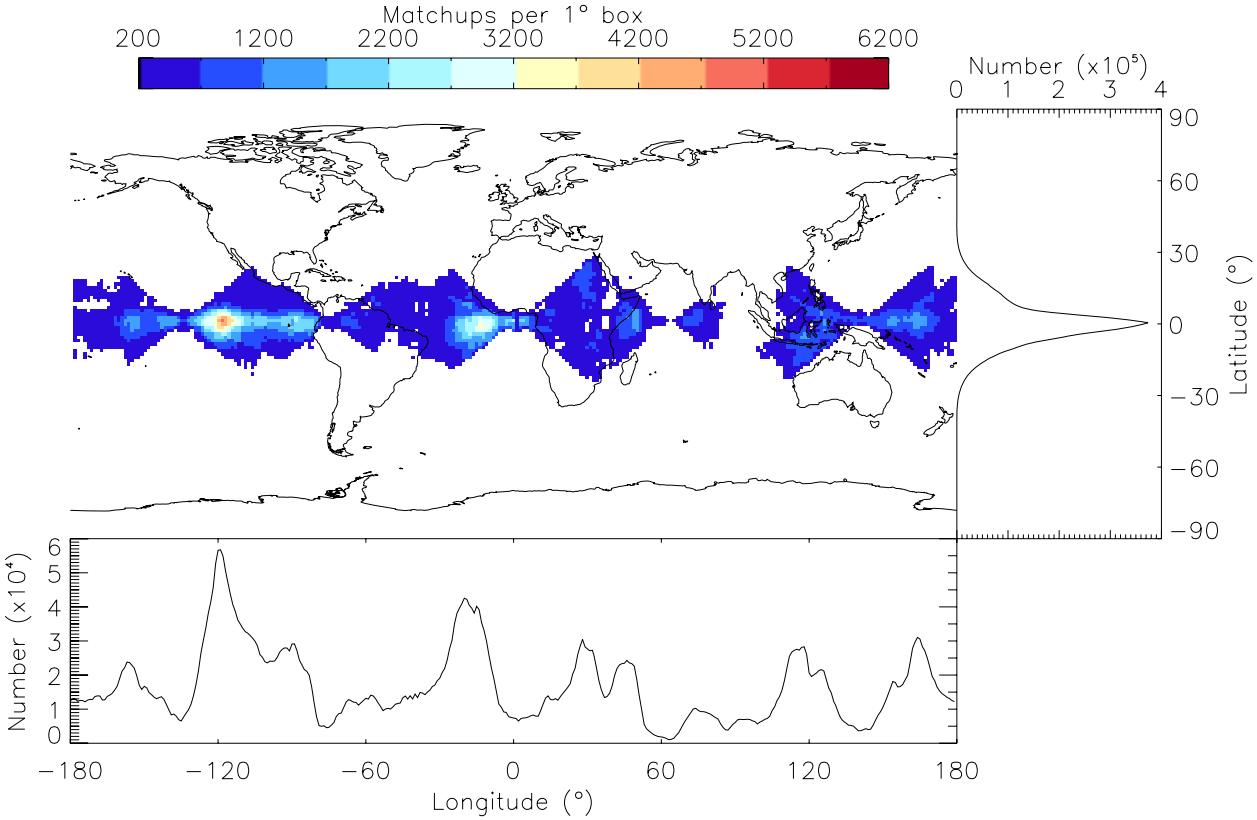

441

442 **Figure 5 – Geographical distribution of all matchup locations (from 1983 through 2005)**

443 **using the initial filter (Table 1).**

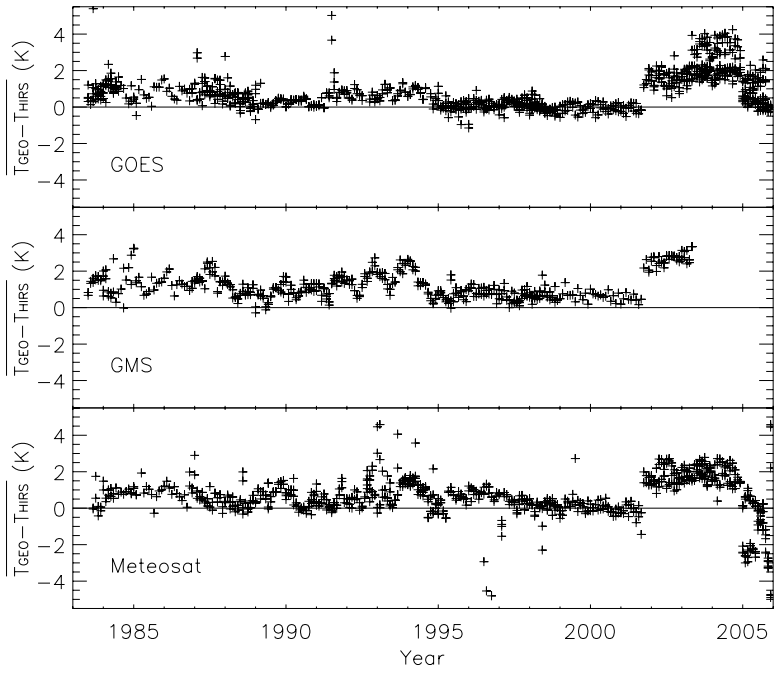

444

445 **Figure 6 – Monthly bias difference grouped by satelite series between T_{GEO} and T_{HIRS} for**

446 **each satellite-month using the initial matchup filter.**

447 A B

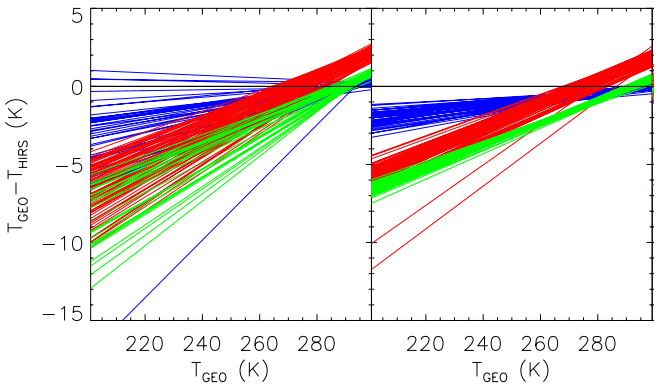

448

449 **Figure 7 – Difference from the one-to-one line for monthly linear regressions of GOES-10**

450 **T_{GEO} with T_{HIRS} for a) the initial filter and b) the proportionate filter. Blue lines are for**

451 **months prior to October 2001, red lines are from Oct. 2001 through December 2004 and**

452 **green lines are months during 2005.**

453 A B

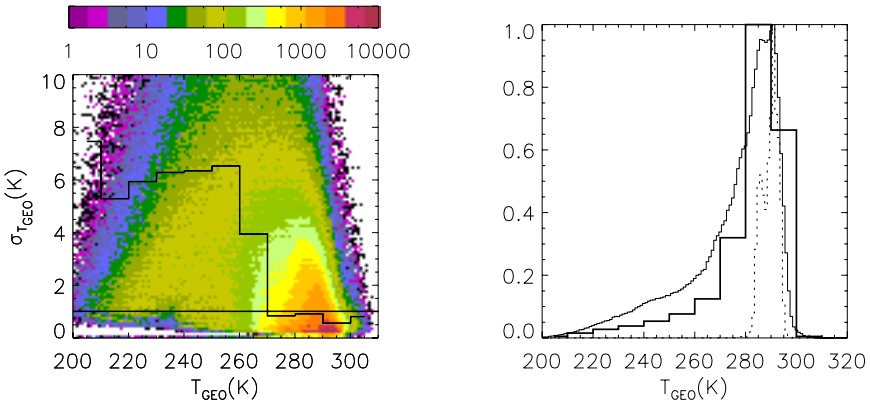

454

455 **Figure 8 - a) Two-dimensional histogram of August 1998 matchups between NOAA-**

456 **12/HIRS and GOES-8 by geostationary spatial noise (σ_T) and T_{GEO}. Solid line at 1K**

457 **represents the initial filter limit and the stepped line represents the new proportionate filter**

458 **limit. b) Normalized distribution of temperature for all matchups (solid line, 1K bins),**

459 **initial filter (dashed line) and the proportionate filter (solid line 10K bins).**

460

461 A B C

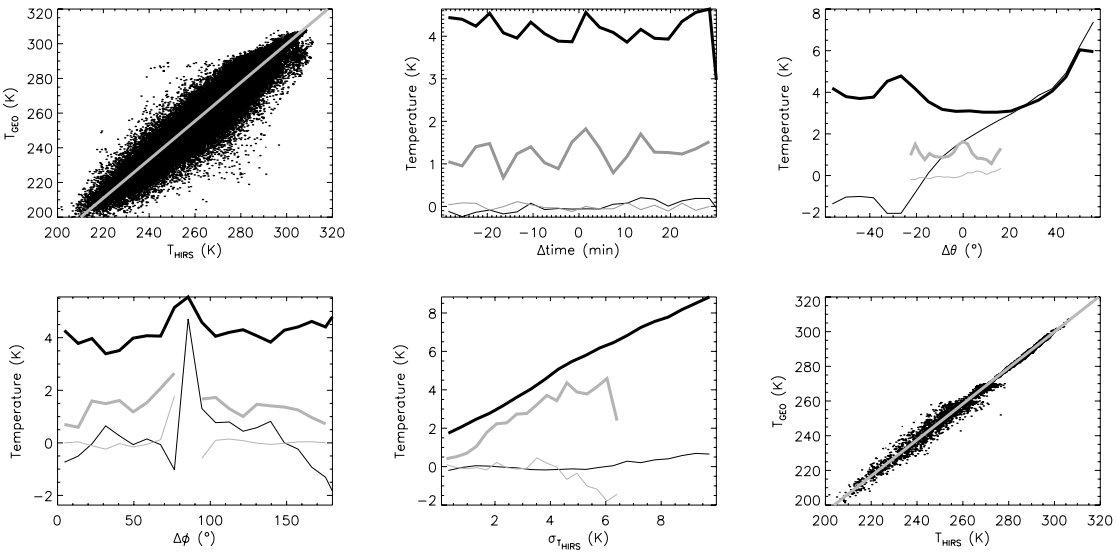

462

463 D E F

464 **Figure 9 – a) TGEO versus T_{HIRS} for all matchup points between NOAA-12/HIRS and**

465 **GOES-8 for August 1998. b-e) Distribution of RMS (thick line) and bias (thin) differences**

466 **for all points (black line) and the proportionate filter (gray line) for difference in b) time, c)**

467 **view zenith angle (θ), d) relative azimuth angle (GREEK PHI) and e) spatial noise of the**

468 **HIRS observations ($σ_T$). f) T_{GEO} versus T_{HIRS} from the proportionate filter.**

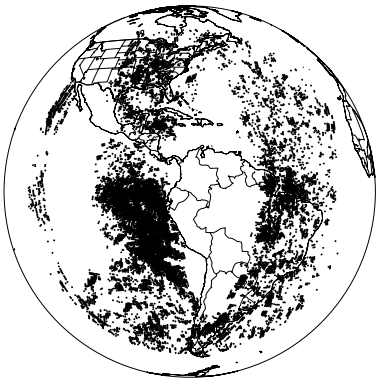

Figure 10 – Spatial distribution of matchup locations for points in Figure 9f using the proportionate filter.

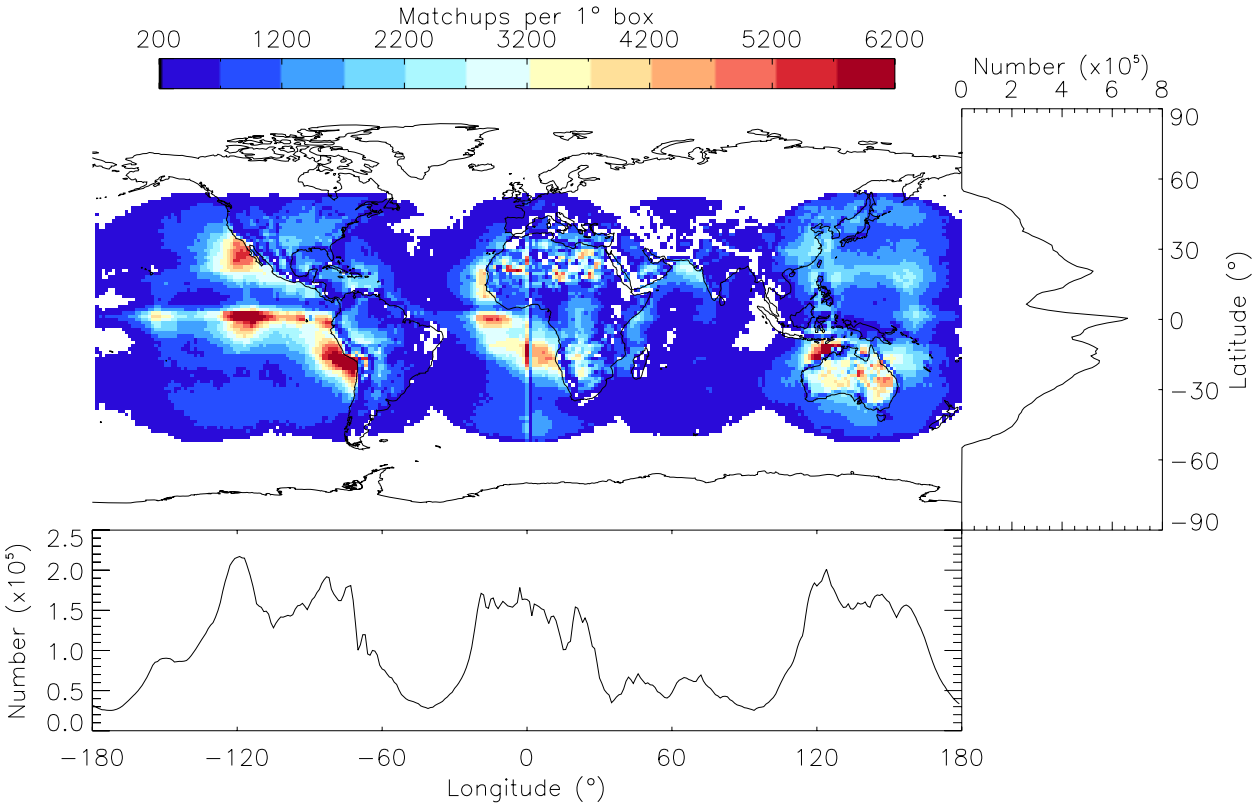

Figure 11 - Same as Figure 5**, but using the proportionate filter (Table 1).**

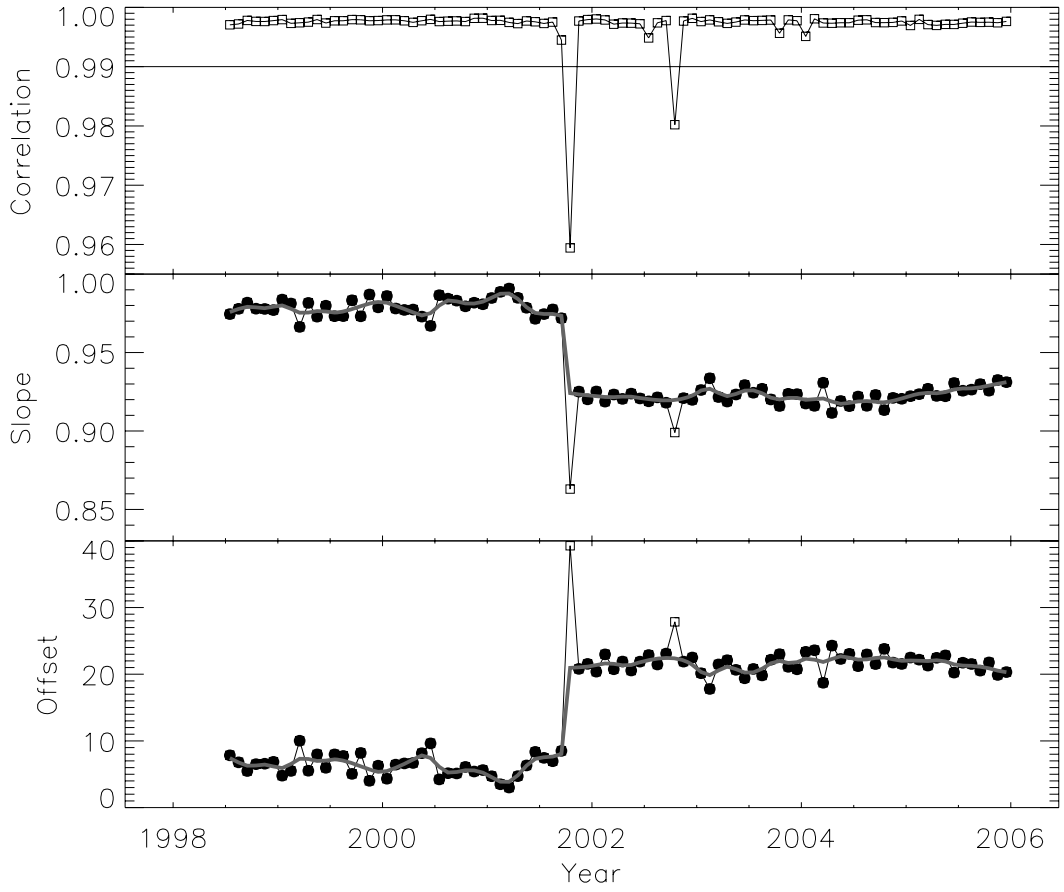

Figure 12 - Time series of linear regression correlation, slope and offset for proportionate-filtered monthly matchups between HIRS and GOES-10 infrared window channel. Months with a correlation above 0.99 were used (solid circles in slope and offset) in the temporal smoothing (gray line) to produce the final calibration correction for the slope and offset values.

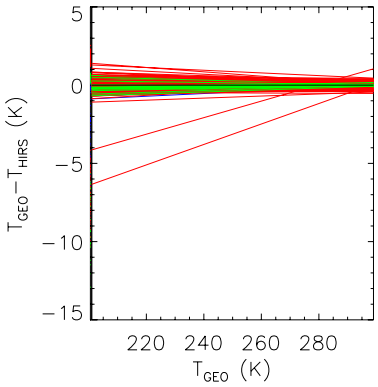

484

485 **Figure 13 – Same as Figure 7 except now using the corrected calibration (blue lines for**

486 **months before October 2001 are obscured by the red and green lines).**

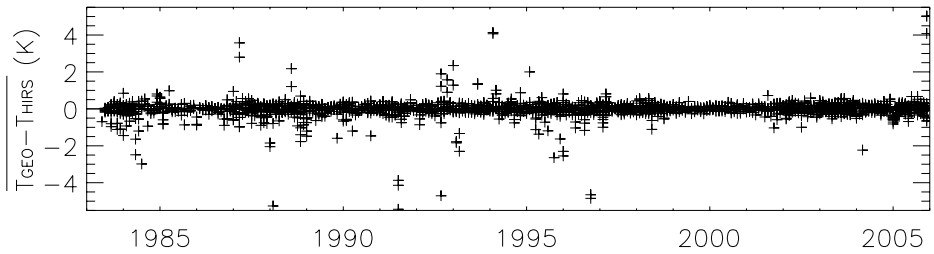

Figure 14 – Monthly bias differences for all geostationary satellites and all months available after calibration correction based on the proportionate filter (cf. Figure 6).